ISSN 1560-0904, Polymer Science, Series B, 2021, Vol. 63, No. 6, pp. 925–932. © Pleiades Publishing, Ltd., 2021.

COMPOSITES

Studies on Electrical, Dielectric and Seebeck Measurement of Polyaniline-Cadmium Oxide Nanocomposite

Ariba Bibi[a,*], Abdul Shakoor[a], Seerat-ul-Arooj[a], and N. A. Niaz[a]

[a] *Department of Physics, Bahauddin Zakariya University, Multan, 60800 Pakistan*

**e-mail: aribaphysics063@gmail.com*

Received March 10, 2021; revised August 8, 2021; accepted August 26, 2021

Abstract—The basic aim of this research work is to synthesize polyaniline and polyaniline-cadmium oxide nanocomposites with different concentrations by using in-situ chemical polymerization methods. The effect of cadmium oxide content on structural and morphological features of the polyaniline matrix are discussed in detail. As the concentration of cadmium oxide in polyaniline matrix augments, then crystallinity of the nanocomposites increases. Two probe methods for temperature dependent dielectric measurements revealed that electrical conductivity of nanocomposites increases with increase in temperature and cadmium oxide content. The response of permittivity to temperature is increased with increasing the cadmium oxide concentration in the nanocomposite and frequency. Four probe methods of Seebeck coefficients exhibit linear increase for nanocomposites with temperature as well as cadmium oxide content.

DOI: 10.1134/S156009042106004X

INTRODUCTION

Owing to their good insulating properties, polymers have exhibited a wide variety of applications [1]. However, in the recent decades, a certain class of polymers exhibited semiconducting behavior [2]. This generation of polymers demonstrated electrical and optical properties of metal or any other semiconductors have numerous technological applications [3]. In material sciences conducting polymers (CPs) have become the main focus of research. Most of the conducting polymers are widely used in chemical sensors, biosensors, organic light emitting diodes, antielectrostatic coating, polymeric solar cell and organic semiconductors [4, 5]. Having alternating single and double bonds or conjugated σ and π bonds along the chain of polymers help the charge delocalization [6]. Among others, polyaniline (PANI) is the favorable conducting polymer due to its high conductivity, ease of the synthesis, low cost, revertible acid base chemistry and environmental stability [7, 8]. Moreover, the introduction of dopants in the polymer matrix increases their conductivity and stability as well [9]. Metal oxide doped CPs exhibited a new range of material with improved properties as compared to metal oxide and pristine conducting polymers [10].

Cadmium oxide (CdO) is an *n*-type semiconductor with profound applications in photodiode [11], transparent electrodes, IR detectors, photovoltaic cells, liquid crystal display and anti-reflection coatings [12]. Doping of PANI with CdO not only enhanced its structural, optical but electrical properties as well as compared to pure aniline [13]. In the modern era of science and technology thermocouple devices have significant applications in temperature sensors, radiation sensors and gas safety equipment [14]. Thermocouples fabricated with alloys, e.g. Ti, Al, W, and Au being expensive and complex synthesis methodologies are not very much attractive.

In the present work, we have synthesized PANI and its nanocomposites with different weight percentage of CdO nanoparticles by in-situ chemical oxidative polymerization of aniline monomer with ammonium persulfate (APS) as an oxidizing agent. The basic aim of production of PANI-CdO nanocomposites is to probe the effect of CdO contents on the structure, morphology, electrical and thermoelectric properties of polyaniline. So that we may incorporate them for the fabrication of electronic devices.

EXPERIMENTAL

Materials and Methods

Aniline ($C_6H_5NH_2$, 99.5%) was purchased from Riedel-de haën. Cadmium Oxide (CdO, 99%) was purchased from Uni-Chєmm. Ammonium persulphate ($(NH_4)_2 S_2O_8$, Duksan, 98%) and hydrochloric acid (HCl, AnalaR, 32%) were used as an oxidant. Double distilled water was used as a solvent in polymerization for the synthesis of PANI and PANI/CdO nanocomposites. All chemicals used in the experiment were of analytical grade.

Synthesis of Polyaniline (PANI)

Polyaniline was synthesized by the in-situ chemical polymerization of aniline monomer in the presence of HCl and APS. 0.5 mol of aniline monomer was dispersed in 100 ml of deionized water. The solution was kept on a magnetic stirrer and 5 mol of HCl dissolved in 200 mL deionized water was added drop wise under vigorous stirring for 1.5 h. Then 0.6125 mol of APS was added drop wise under vigorous stirring, the color of the mixture changes and the reaction mixture was kept at room temperature for one day. Finally, the suspension was filtered and washed with de-ionized water several times and then washed with methanol. The greenish paste of polyaniline was obtained and dried under sunlight for 2–3 h [15]. Finally, the resultant product was kept in vacuum oven for 24 h at 60°C.

Synthesis of PANI-CdO Nanocomposites

0.5 mol of aniline monomer was dispersed in 100 mL of deionized water. The solution was kept on a magnetic stirrer and 5 mol of HCl dissolved in 200 mL deionized water was added drop wise under vigorous stirring for 1.5 h. Then 0.6125 mol of APS was added drop wise under vigorous stirring and 10 wt% of CdO was also added to the solution, until the CdO suspended in the solution. The color of the mixture changes and the reaction mixture was kept at room temperature for one day. Finally, the suspension was filtered and washed with de-ionized water several times and then washed with methanol. The greenish paste of polyaniline was obtained and dried under sunlight for 2–3 h. Finally, the resultant product was kept in vacuum oven for 24 h at 60°C. Thorough grinding was carried out in an agate mortar and pestle. Similarly, PANI-CdO 20% was synthesized.

Measurements

Electronic properties (dielectric and conductivity) were studied by using two-probe technique in the frequency range 10^2–10^6 Hz in LCR Meter Model 8101 and temperature range 303–423 K. X-Ray powder diffraction analysis was carried out using an automated diffractometer, Advance model D8 equipped with CuK_α radiations (λ = 1.54 Å). The instrument was operated at 40 kV and 30 mA and the samples were mounted on a standard holder. The diffracted patterns were recorded over the range of 10°–80° and counting time was 0.5 s and the step size 0.02. Scanning electron microscopy (SEM) was carried out by using an EVO50 ZEISS instrument. The ground powders of composite materials were pressed into the disk shaped pellets of pristine PANI and its composites with CdO were formed by using a press machine at 10 ton pressure in stainless steel die of 1 mm thickness and 13 mm diameter. Conducting silver paste was applied to the pellets of synthesized composites to serve as electrodes in contact with the two circular faces. The pellet was then held between two spring loaded copper plates. For the Seebeck coefficient measurement, in which one end of the sample is held at affixed temperature while the other end is varied through temperature T. The slope of the linear relationship between the thermoelectric voltage ΔV and the temperature difference ($\Delta T \approx$ 10 K) was then used to calculate the Seebeck coefficient ($S = \Delta V/\Delta T$) [16].

RESULTS AND DISCUSSION

Figure 1a represents XRD spectra of pristine CdO which indicates the monoclinic peaks observed at 2θ = 33.06°, 38.35° and 55.32° corresponding to the (111), (200) and (220) planes with d-values 2.706, 2.346, 1.640 Å. XRD spectra of pure CdO signifies the crystalline nature of CdO [17]. All the peaks in XRD pattern are well matched with the JCPDS card numbers 05-0640 and 73-2245. Figure 1b represents XRD pattern of PANI and its nanocomposites with CdO. Figure 1b (curve *1*) gives the broad peak in 2θ range 17.5°–28° which correspond to the characteristic band of PANI homopolymer [18]. This suggests the amorphous nature of polyaniline. Figure 1b represents XRD spectra of PANI-CdO, in which spectral peaks were observed at 2θ = 33.5°, 37.5°, and 53.5° corresponding to the planes (111), (200) and (220) respectively. It may be concluded that as the CdO content increases then crystallinity of nanocomposites also increases. As the cadmium oxide is a polycrystalline material, so there must be the possibility for PANI to grow in the basal plane of CdO [19]. It is obvious from Figure 1b that CdO maintains its crystalline nature even after uniform dispersion in PANI throughout polymerization reaction [20].

Morphology of hybrid composite is a crucial factor for the electronic properties of polymers. Figure 2 shows the comparison of SEM images of PANI (Fig. 2a), PANI loaded with 10% CdO (Fig. 2b), PANI loaded with 20% CdO (Fig. 2c) and pristine CdO (Fig. 2d). The SEM image in Fig. 2a shows that pure PANI has the branched like irregular morphology and sponge structure with deep pores [17]. The SEM images depicted in Figs. 2b, 2c indicates that the incorporation lead to homogenously distributed CdO into the polymer matrix [21]. The final samples appear as agglomerated macromolecules having spherical and porous structure. Figure 2d depicts the agglomerated and spherical structure of CdO. By increasing the concentration of CdO in PANI, granular structure increases and porosity decreases [20].

The dielectric parameter as a function of frequency was described by the complex permittivity in the form:

$$\varepsilon^*(f) = \varepsilon'(f) - i\varepsilon''(f), \quad (1)$$

where the real part ε' and imaginary part ε'' are the components for the dielectric constant and dielectric loss respectively.

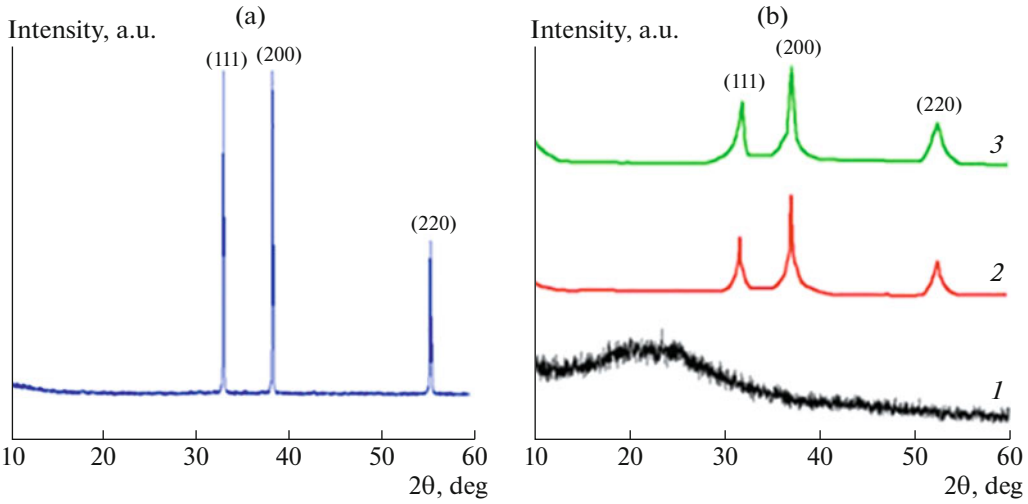

Fig. 1. (a) XRD pattern of pristine CdO, (b) (*1*) pristine PANI, (*2*) PANI-CdO 10%, (*3*) PANI-CdO 20%.

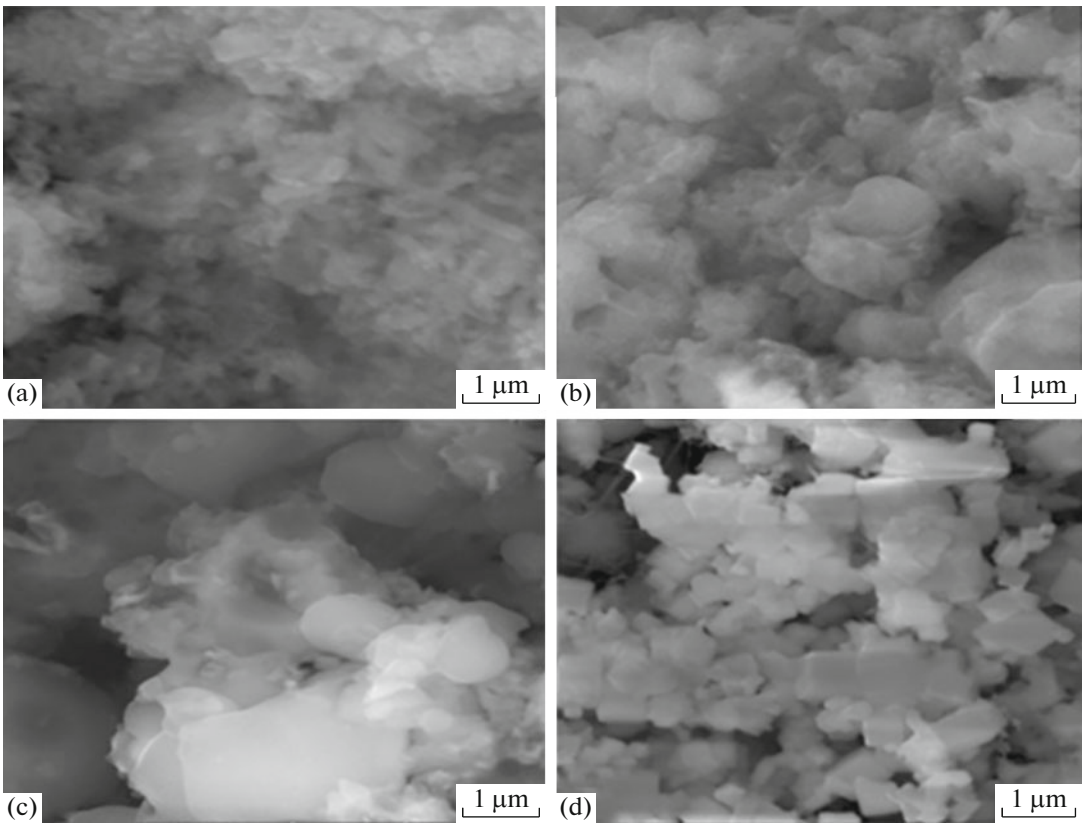

Fig. 2. SEM of (a) pristine PANI, (b) PANI-CdO 10%, (c) PANI-CdO 20%, (d) pure CdO.

The dielectric constant was calculated by the Eq. (2), where ε' is dielectric constant, d is the thickness of the sample, A is area of cross section. If C_p is the equivalent parallel capacitance and $C_o = (0.08854 \times A/d)pF$, is the geometrical capacitance in vacuum with the same dimensions as that of the sample.

$$\varepsilon' = \frac{C_p}{C_o}. \quad (2)$$

The measured conductance G was taken to calculate the dielectric loss, ε'' using the following expression:

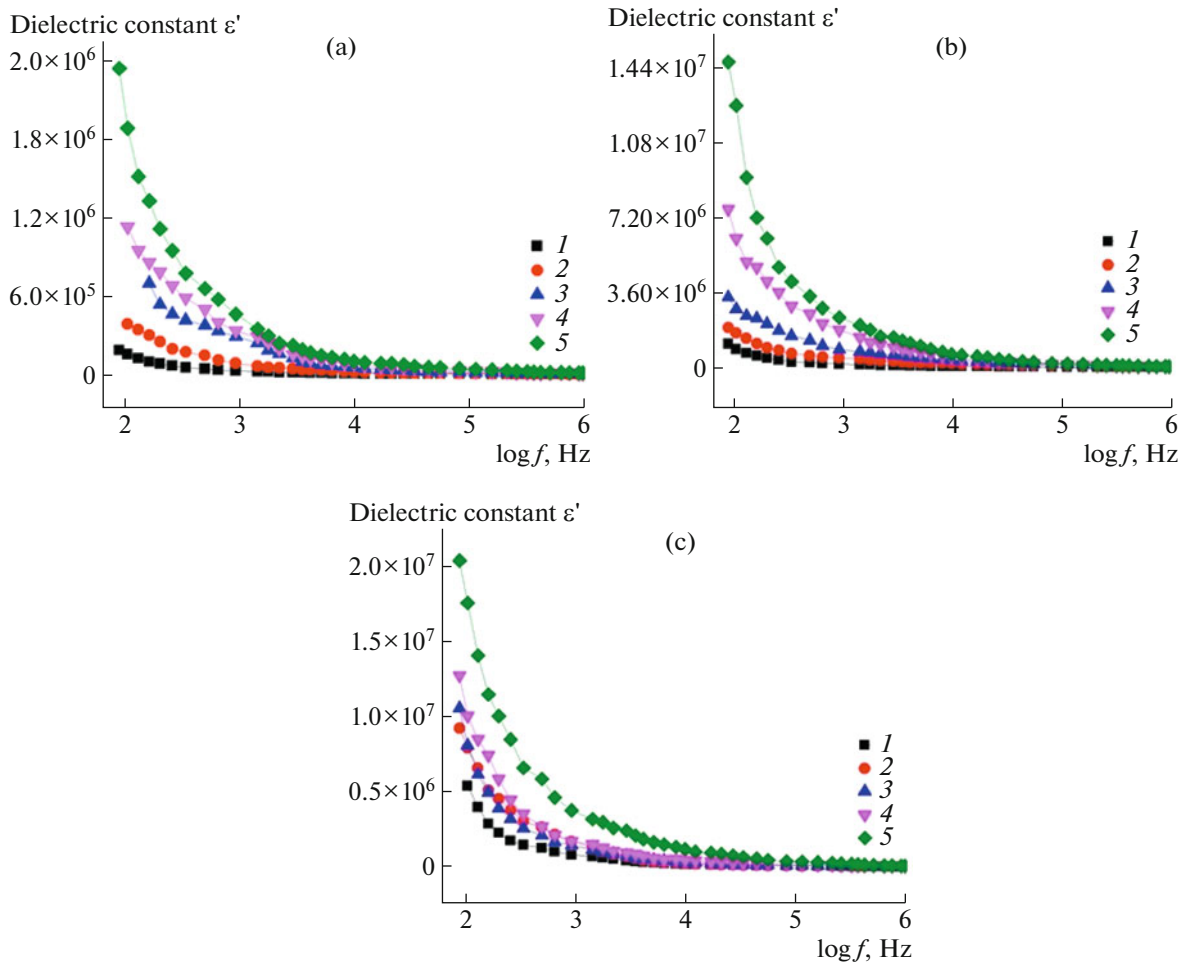

Fig. 3. Dielectric constant variation as a function of frequency of (a) pristine PANI, (b) PANI/10% CdO, and (c) PANI/20% CdO at (*1*) 303, (*2*) 333, (*3*) 363, (*4*) 393, (*5*) 423 K.

$$\varepsilon'' = G\left(\frac{d}{\epsilon_0 \omega A}\right) = \varepsilon' D, \quad (3)$$

where angular frequency, $\omega = 2\pi f$, f—frequency and ϵ_0—permittivity in free space.

Figure 3 shows the dielectric constant of pristine PANI and PANI/CdO nanocomposites versus frequency at different temperatures. The overall trend of the dielectric behavior of all the composites decreases with increase in the applied AC frequencies. This is as expected in the case of conducting polymer composites [22–25]. All the nanocomposites show a reasonable dielectric property with frequency and temperature. All the materials show higher values of dielectric constant at low frequency and high temperature. Beyond a certain frequency, the materials show a sudden drop in the magnitude of ε' and are indifferent to temperature.

Across all the composites, composites having higher content of CdO (20%) exhibit higher ε' value compared to the composites with lower content (10%) and pristine PANI, and it is attributed to the enhanced surface area that arises from the interfacial adhesion between CdO and PANI matrix. The magnitude of ε' of nanocomposites essentially reveals that system exhibits strong interfacial polymerization at low frequency. Interfacial polarization occurs when there is an accumulation of charge between the two conductive and insulating regions within the material when electric field is applied [26]. The decreasing ε' with the increasing frequency (viz., at high enough frequency) is attributed to the dielectric relaxation [27], the variation in the field is very rapid for the dipoles to align themselves hence results in less dielectric constant.

In dielectric analysis, dielectric constant regime at low frequencies is attributed to the interfacial polarization and DC conductivity while at higher frequencies; regime is associated with dipolar relaxation [22].

Figure 4 shows the dielectric loss behavior of pristine PANI and PANI/CdO nanocomposites versus frequency at different temperatures.

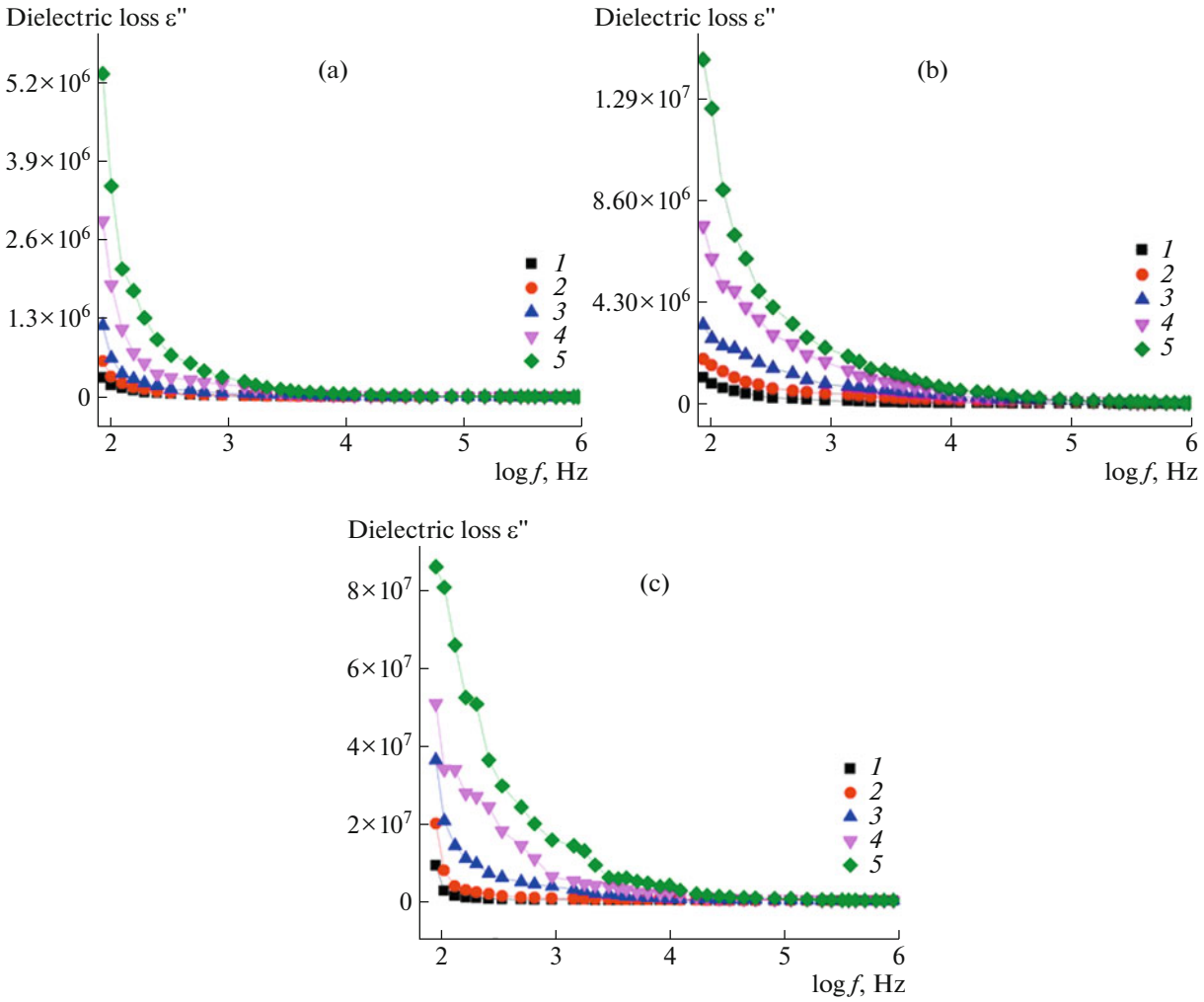

Fig. 4. Dielectric loss variation as a function of frequency of (a) pristine PANI, (b) PANI/10% CdO, and (c) PANI/20% CdO at (*1*) 303, (*2*) 333, (*3*) 363, (*4*) 393, (*5*) 423 K.

The dielectric loss is a combination of three distinct effects:

$$\varepsilon''(\omega) = \varepsilon''(\omega)_{DC} + \varepsilon''(\omega)_{IP} + \varepsilon''(\omega)_{D}, \qquad (4)$$

where $\varepsilon''(\omega)_{DC}$ is due to DC conduction, $\varepsilon''(\omega)_{IP}$ is due to interfacial polarization and $\varepsilon''(\omega)_{D}$ is due to oriental polarization (Debye type). The high value of dielectric loss at low frequencies is mainly due to DC conduction and interfacial polarization [28]. It is observed that both dielectric constant and dielectric loss increases with increase in temperature. This is because as the temperature of the sample increases, the dipoles comparatively become free and they respond to the applied electric field. Hence, polarization increases which leads to increase in dielectric constant [29, 30].

Figure 5 shows the AC conductivity of pristine PANI and PANI/CdO nanocomposites versus frequency at different temperatures.

The measured conductance G from 10^2 Hz to 1 MHz was considered to calculate the AC conductivity σ_{ac} using the following expression:

$$\sigma_{ac} = G\left(\frac{d}{A}\right) = \omega\varepsilon''\epsilon_o, \qquad (5)$$

where d is the thickness of the sample and $A = \pi r^2$ is the cross-sectional area of the pellets of sample, r is the radius of the pellet.

The real part of the conductivity σ_{ac} exhibits the features of AC conductivity in disordered materials with two distinct regimes separated by the critical frequency f_c. At low applied AC frequencies, the conductivity σ_{ac} is almost constant which corresponds to the DC conductivity σ_o such that

$$\sigma_{ac} \approx \sigma_o, \quad \text{where} \quad f < f_c. \qquad (6)$$

At higher frequencies, σ_{ac} increases with the applied AC frequency in accordance with the hopping

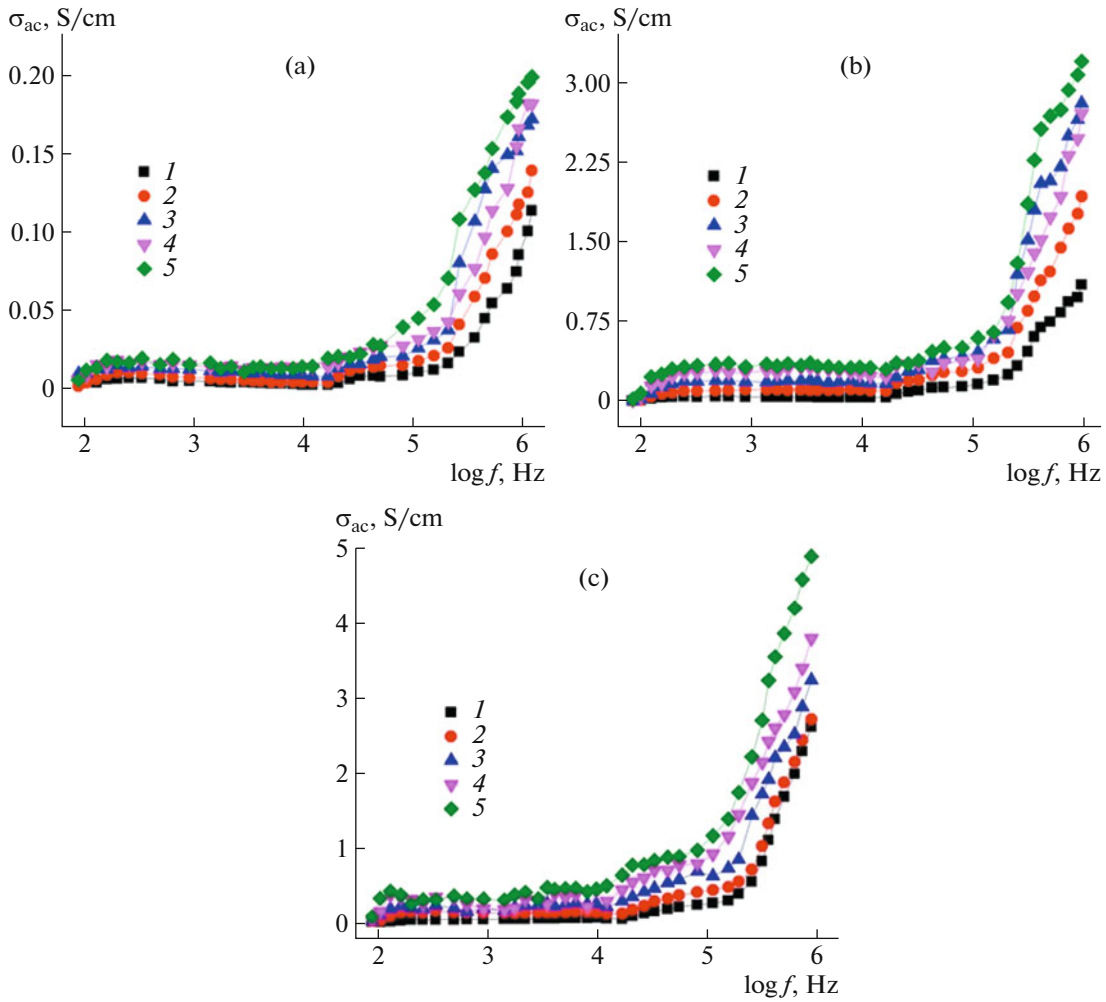

Fig. 5. AC conductivity of (a) pristine PANI, (b) PANI/10% CdO, and (c) PANI/20% CdO at (*1*) 303, (*2*) 333, (*3*) 363, (*4*) 393, (*5*) 423 K.

model of charge transport in disordered materials. The conductivity behavior can be approximated by a power law given by [33]:

$$\sigma_{ac} = A\omega^{s}, \quad \text{where} \quad 0 < s < 1, \tag{7}$$

where s is the frequency exponent and A is the pre-exponential factor. Critical frequency f_c is not a well-defined parameter, and it depends on various factors like method of synthesis, composition and microstructure formation etc.

It is evident from the figure that the AC conductivity is frequency-dependent and is enhanced with increase in the frequency [31], also depends upon the crystallinity, nature of filler particles, polarity of polymer and temperature [32]. It is also observed that AC conductivity remains constant at low frequencies and as frequency increases the conductivity increases exponentially. At all temperatures it is observed that above 100 kHz, σ_{ac} increases exponentially. This frequency is called the critical frequency. AC conductivity obeys the power-law well above the critical frequency for the composite.

It is noteworthy that the conductivity increases as content of CdO increases. The increase in ac conductivity with the addition of CdO in the composite may be attributed to the extended hopping of charge carriers. Presence of CdO in PANI matrix has enhanced the electrical properties in the composites. This may be attributed to charge polarization effects. Distribution of CdO in the composite is homogenous and favored most of the charge carriers to polarize at the specified localized sites leading to the improved conductivity. Table 1 shows ac conductivity and dielectric parameters of PANI and its CdO composites.

Figure 6 (curve *1*) depicts the variation of seebeck coefficients with temperature of pristine PANI while Fig. 6 (curves *2*, *3*) displays the variation of Seebeck coefficients with temperature of 10 and 20% PANI respectively. Positive values of Seebeck coefficient indicate that bulk of conduction is due to the majority

Table 1. Calculation of conductivity and dielectric parameters at various concentrations of CdO in PANI.

Sample	Dielectric constant at 100 Hz and room temperature	Dielectric loss at 100 Hz and room temperature	AC conductivity at 1 MHz and room temperature, S/cm
Pristine PANI	1.95×10^5	3.20×10^5	0.11
PANI/10%CdO	1.13×10^6	1.13×10^6	1.09
PANI/20%CdO	9.24×10^6	9.07×10^6	2.62

charge carriers, holes, which originate from the p-type semi-conducting materials. Seebeck coefficient increases linearly with the increase in temperature expressing the diffusive metallic thermopower behavior [34]. Seebeck coefficient increases as increasing the CdO concentration may be ascribed due to the large number of interfaces between the polyaniline and CdO phases [35]. Seebeck coefficient of the composite increases due to the high coordination polymer content [36]. Maximum values of seebeck coefficients at 423 K for pristine PANI, PANI/10%CdO and PANI/20%CdO are 31, 37, and 41 μV/K respectively.

CONCLUSIONS

Polyaniline and PANI-CdO composites with different weight percentages have been synthesized successfully by in-situ chemical polymerization methods. The structural characterization of PANI and its nanocomposite reveals the well incorporation of the cadmium oxide in the PANI matrix. The microstructural analysis (SEM) depicts that PANI and its nanocomposite formed agglomerated macromolecules and have spherical structure that is also confirmed from XRD.

Polymer nanocomposites exhibit higher values of both dielectric constant and dielectric loss with increase in the temperature and decrease in frequency. AC conductivity obeys the power-law well above the 100 kHz frequency for the nanocomposites and increases exponentially for all temperature variations. It has been noticed that variation in temperature on PANI/CdO composite showed a prominent effect on dielectric properties and conductivity. Seebeck analysis of PANI and its composite suggests that by increasing temperature seebeck coefficient increases and also depend upon the carrier concentration. The enhanced electrical conductivity for the composites of PANI with 10 and 20% of CdO with ordered structure compared to pure PANI may be applicable in electronic devices and thermocouple such as the temperature sensors, thermistors, radiation sensors, flame sensors in safety devices.

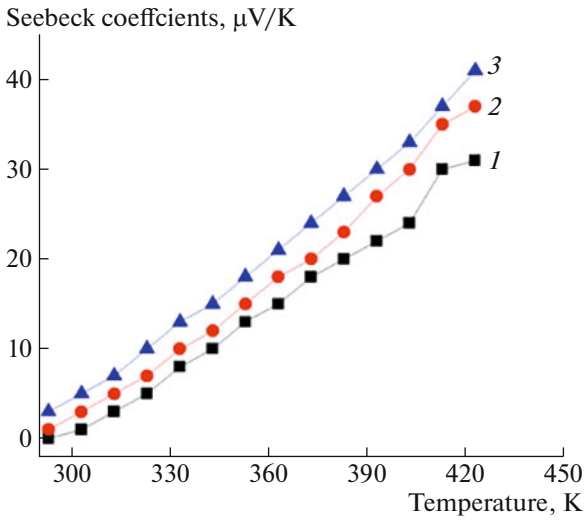

Fig. 6. Seebeck coeffcients vs temperature (*1*) PANI, (*2*) PANI/10% CdO, (*3*) PANI/20% CdO.

CONFLICT OF INTEREST

The authors declare that they have no conflict of interest.

REFERENCES

1. V. R. Gowariker and N. V. Viswanathan, J. Sreedhar, AlChE J. **33**, 2097 (1986).
2. M. V. Murugendrappa, A. Parveen, and M. V. N. Ambika Prasad, Mater. Sci. Eng., A **459**, 371 (2007).
3. V. Saxena and B. D. Malhotra, Curr. Appl. Phys. **3**, 293 (2003).
4. U. Lange, N. V. Roznyatovskaya, and V. M. Mirsky, Anal. Chim. Acta **614**, 1 (2008).
5. K. Guerchouche, E. Herth, L. E. Calvet, N. Roland, and C. Loyez, Microelectron. Eng. **182**, 46 (2017).
6. M. Amita, K. Kiruthiga, S. Mahalakshmi, V. Parthasarathy, C. Hu, Yi-F. Lin, K. L. Tung, and R. Anbarasan, J. Sol-Gel Sci. Technol. **91**, 611 (2019).
7. G. Gustafsson, Y. Cao, G. M. Treacy, F. Klavetter, N. Colaneri, and A. J. Heeger, Nature **357**, 477 (1992).
8. M. J. Sailor, E. J. Ginsburg, C. B. Gorman, A. Kumar, R. H. Grubbs, and N. S. Lewis, Science **249**, 1146 (1990).
9. A. S. Roy, K. R. Anilkumar, and M. V. N. Ambika, Ferroelectrics **413**, 279 (2011).
10. S. B. Kondawar, S. R. Thakare, V. Khati, and S. Bompilwar, Int. J. Mod. Phys. B **23**, 3297 (2009).
11. M. Soylu and H. S. Kader, J. Electron. Mater. **45**, 5756 (2016).
12. S. Ilican, M. Caglar, and Y. Caglar, Optoelectron. Adv. Mater., Rapid Commun. **3,** 135 (2009).

13. S. Kondawar, R. Mahore, A. Dahegaonkar, and S. Agrawal, Adv. Appl. Sci. Res. **2**, 401 (2011).
14. G. E. Daniels, J. App. Meteorol. **7**, 1026 (1968).
15. T. Khursheed, M. U. Islam, M. A. Iqbal, I. Ali, A. Shakoor, M. S. Awan, A. Iftikhar, M. A. Khan, and M. N. Ashiq, J. Magn. Magn. Mater. **393**, 8 (2015).
16. C. Wood, A. Chmielewski, and D. Zoltan, Rev. Sci. Instrum. **59**, 951 (1988).
17. R. Paulraj, P. Shankar, G. K. Mani, L. Nallathambi, and J. B. B. Rayappan, J. Electron. Mater. **47**, 6000 (2018).
18. L. Aijie, B. L. Huu, K. Ji-Soon, K. Byoung-Kee, and K. Jin-Chun, J. Nanosci. Technol. **13**, 7728 (2013).
19. A. S. Aldwayyan, F. M. Al-Jekhedab, M. Al-Noaimi, B. Hammouti, T. B. Hadda, M. Suleiman, and I. Warad, Int. J. Electrochem. Sci. **8**, 10506 (2013).
20. A. S. Roy, K. R. Anilkumar, and M. V. N. Ambika Prasad, J. Appl. Polym. Sci. **123**, 1928 (2012).
21. A. S. Roy, K. R. Anilkumar, and M. V. N. Ambika Prasada, Ferroelectrics **413**, 279 (2011).
22. Y. Ravikiran, M. Lagare, M. Sairam, N. Mallikarjuna, B. Sreedhar, S. Manohar, A. MacDiarmid, and T. Aminabhavi, Synth. Met. **156**, 1139 (2006).
23. R. D. Balikile, A. S. Roy, S. C. Nagaraju, and G. Ramgopal, J. Mater. Sci.: Mater. Electron. **28**, 7368 (2017).
24. T. Machappa and M. V. N. A. Prasad, Ferroelectrics **392**, 71 (2009).
25. T. Machappa and M. V. N. A. Prasad, Phys. B (Amsterdam, Neth.) **404**, 4168 (2009).
26. N. Pinto, A. Acosta, G. Sinha, and F. Aliev, Synth. Met. **113**, 77 (2000).
27. J. Zhu, S. Wei, L. Zhang, Y. Mao, J. Ryu, N. Haldolaarachchige, D. P. Young, and Z. Guo, J. Mater. Chem. **21**, 3952 (2011).
28. B. G. Soares, M. E. Leyva, G. M. Barra, and D. Khastgir, Eur. Polym. J. **42**, 676 (2006).
29. X. Yan and T. Goodson, J. Phys. Chem. B **110**, 14667 (2006).
30. N. N. Mallikarjuna, S. K. Manohar, P. V. Kulkarni, A. Venkataraman, and T. M. Aminabhavi, J. Appl. Polym. Sci. **97**, 1868 (2005).
31. L. N. Shubha and P. Madhusudana Rao, J. Adv. Dielectr. **06**, 1650018-1 (2016).
32. T. Sampreeth, M. A. Al-Maghrabi, B. K. Bahuleyan, and M. T. Ramesan, J. Mater. Sci. **53**, 591 (2018).
33. J. Bisquert and G. G. Belmonte, Russ. J. Electrochem. **40**, 352 (2004).
34. H. Badr, I. S. El-Mahallawi, F. A. Elrefaie, and N. K. Allam, Appl. Phys. A: Mater. Sci. Process. **125**, 524 (2019).
35. L. Wang, D. Wangб and G. Zhu, J. Li, and F. Pan, Mater. Lett. **65**, 1086 (2011).
36. R. Mulla and M. K. Rabinal, ACS Comb. Sci. **18**, 177 (2016).